IEEE Access
Multidisciplinary ⋮ Rapid Review ⋮ Open Access Journal

Received December 19, 2020, accepted January 10, 2021, date of publication January 19, 2021, date of current version January 28, 2021.

Digital Object Identifier 10.1109/ACCESS.2021.3052892

SDN Wireless Controller Placement Problem-The 4G LTE-U Case

AVIRAM ZILBERMAN[1], YORAM HADDAD[2], (Senior Member, IEEE), SEFI ERLICH[1], YOSSI PERETZ[2], AND AMIT DVIR[1]

[1]Ariel Cyber Innovation Center, Department of Computer Science, Ariel University, Ariel 4077625, Israel
[2]Department of Computer Science, Jerusalem College of Technology, Jerusalem 91160, Israel

Corresponding author: Amit Dvir (amitdv@g.ariel.ac.il)

This work was supported by the Neptune consortium.

ABSTRACT To cope with the shortage of available licensed spectrum, 4th Generation Long Term Evolution (4G LTE) is expected to be deployed also in the unlicensed spectrum. This raises the problem of the coexistence of multiple operators. Obviously, a Software Defined Networking (SDN) based control approach can utilize the radio bandwidth by coordinating between multiple LTE-Unlicensed (LTE-U) operators. Within SDN control plane, there is a well-known issue namely the Controller Placement Problem (CPP) which has a major impact on the efficiency of the control plane. This paper addresses the Wireless Controller Placement Problem (WCPP) when the SouthBound interface (SBi) is based on 4G LTE unlicensed. The proposed solution improves the throughput, link failure probability and the transparency on the SBi from concurrent transmissions on the control plane. Two heuristic solutions are considered, one is a simulated annealing based and the other is a ray-shooting based. The simulation results show that they are fast and efficient and the ray-shooting based heuristic out-performs the simulated annealing based heuristic. In addition, it is shown that the transparency improves in bigger networks.

INDEX TERMS LTE, placement, SDN, simulated annealing, wireless, stochastic geometry.

I. INTRODUCTION

The rapid proliferation of media-rich mobile devices has brought a dramatic increase in mobile data traffic. The main solutions to the rapid increase in traffic are: i) increased spectral efficiency through advanced physical and MAC layer techniques to support more bits/s/Hz per node [1]; ii) network densification via deployment of more small cells to improve the area spectral efficiency [2]; iii) addition of more radio spectrum to increase bandwidth [3].

Licensed spectrum can provide predictable high-quality services with high spectral efficiency, but the need for more licensed spectrum is never-ending [4]. However, the licensed spectrum below 6 GHz is limited. Hence, there is increasing interest on the part of mobile operators to leverage unlicensed spectrum.

Even though unlicensed spectrum has been used to offload data traffic via Wi-Fi networks, Long Term Evolution (LTE) in unlicensed spectrum (LTE-U) with the 4G-LTE radio communications technology enables mobile operators to make efficient use of unlicensed spectrum while managing a unified radio network. This provides new opportunities to alleviate spectrum scarcity and boost network capacity. In contrast to licensed spectrum, unlicensed spectrum is open to different kinds of Radio Access Technologies (RATs) as long as they comply with the regulations [5].

For instance, the introduction of LTE-U will inevitably contend with Wi-Fi for access to the unlicensed spectrum. Due to the lack of inter-RAT compatibility generated by the different RAT specifications (i.e., a centralized scheduling protocol in LTE and a different MAC protocol based on the Distributed Coordination Function (DCF) in Wi-Fi), no information exchange, and asynchronous operation, the co-channel deployment of multiple RATs will cause increased interference to each other and potential degradation of the overall system performance.

In the literature, coexistence between multiple RATs has been discussed for the licensed spectrum [6], [7]. Striving to overcome these challenges, the LTE-U forum was formed by Verizon, Alcatel-Lucent, Ericsson, Qualcomm, and Samsung in 2014 and generated the technical specifications based on the 3rd Generation Partnership Project (3GPP) Rel. 10/11/12,

The associate editor coordinating the review of this manuscript and approving it for publication was Usama Mir.

including coexistence specifications and minimum performance specifications for operating LTE-U base stations and consumer devices [8]. It targets early deployment in countries without Listen-Before-Talk (LBT) requirements, such as US, China and Korea.

The initial LTE-U specifications only focus on Supplemental DownLink (SDL) operations, where the unlicensed spectrum is used solely for downlink transmission. To support coexistence and fair sharing of the unlicensed band, the LTE-U forum specified three solutions: opportunistic SDL, channel selection, and time-domain operation using Carrier Sensing Adaptive Transmission (CSAT).

In opportunistic SDL operation, the unlicensed spectrum will be available when there is no user in the coverage or there is no data in the buffer for users in the coverage. Channel selection can effectively avoid interference in low to medium density scenarios by selecting a clean channel based on channel measurements. The performance of random channel selection was analyzed in [9] which proposed channel selection for LTE-U by randomly selecting one channel unoccupied by Wi-Fi.

Software Defined Networking (SDN) has recently evolved as a new concept to simplify network architecture by separating and centralizing the control functionality from the data forwarding path of networking devices. To date SDN has mainly been applied to cellular networks to reduce the signaling load and is also gaining significance for resource management in interference, capacity limited access and backhaul networks. Meanwhile, there are increasing efforts to adapt SDN to the cellular world. For instance the Open Networking Foundation (ONF) designed a framework to modify the standard South-Bound interface (SBi) called OpenFlow to support mobile networks. In addition, many recent studies have been devoted to leveraging SDN concepts to improve traffic handling, mobility management, and overhead reduction in cellular networks [10], [11].

The rapid growth of networks requires a flexible architecture between the controllers and the switches, but cannot be guaranteed by wired networks. The wireless medium can provide the required flexibility by deploying the network infrastructure (SBi) and adjusting it to changes in loads. However, the shared wireless medium behaves differently from the wired one since it is vulnerable to radio interference, noise, fading signals and other RF phenomena. For example, in a wired SDN, the latency on the SBi is based on the Euclidean distance of the multi-hop path between the switch and its assigned controller, whereas models for latency in wireless networks require a good understanding of the wireless propagation effects and are generally very involved (such as probabilistic models like Rayleigh or Rice's fading models [12]). In addition, the performance of the wireless network is measured by factors that do not exist in a wired network, such as link failure probability that is negligible in wired networks.

In the context of SBi optimization, one of the major (and still open) issues is the Controller Placement Problem (CPP) which was first defined by Heller *et al.* [13]. It is a dominant research issue in the architecture of the control plane. The CPP focuses on the structure of the control plane; i.e., the number of controllers, their locations and the assignment function of the data plane switches to controllers.

This paper extends our previous work [14] and proposes a solution to the CPP in the case of LTE-U networks (LTE-U-CPP), by taking the complexities of the wireless medium between the control plane and the data plane into account and considering the model of two coexisting cellular LTE-U operators that share the common unlicensed bands. An architecture is proposed in which the controllers communicate with the evolved Node Bs (eNBs) of the data plane through LTE-U channels.

To investigate the efficiency of the wireless control plane, an objective function is proposed which is a weighted sum of three objectives: spatial throughput, spatial link failure probability and transparency. The transparency is a new metric that is defined as the marginal latency on the data plane caused by the co-channel interference that is added by the control plane. The relation between the aforementioned metrics and the initial controllers placement is shown by simulations.

The contribution of this work is as follows:

1) A novel model for the metrics of the LTE-U-CPP that are specific to the cellular SDN i.e., throughput and link failure probability on the SBi.
2) An objective function for the LTE-U-CPP (Section V) consisting of the weighted sum of the spatial throughput, spatial link failure probability and transparency..
3) An analysis and use of simulations to show the relationship between the wireless metrics on the SBi and the placement of the control plane.
4) A simulation of the two proposed heuristic algorithms and a demonstration of their efficiency.

The remainder of this paper is organized as follows. Section II lists the existing solutions for the wired and wireless SDN placement problem. Section III presents the network model and Section IV describes the prformance metrics. In Section V the LTE-U Controller Placement Problem is introduced and a detailed model description is proposed. Later on in this section the objective function and the constraints are proposed. Then in Section VI the heuristics for solving the objective function are presented, and in Section VII the simulations that were conducted are shown and a discussion about the outcomes is provided. Section VIII concludes with a few remarks and suggestions for further research.

II. RELATED WORK

This section reviews the state of the art in solving the CPP. The difference between existing solutions lies mainly in the metrics that affect the control plane performance such as the latency of packet transmission on the SBi and the resiliency of the control plane. For instance, in [15] the controllers are located as close as possible to the switches to decrease the latency on the SBi, whereas in [16] the latency calculations

considered the backup routes to increase resiliency, so that the controllers were placed differently. In both cases the latency depended solely on the Euclidean distance because the SBi was a wired interface.

Recently, there has been increasing interest in a wireless SBi in which the controllers communicate with the data plane switches over a wireless channel. Mazied *et al*. [17] claimed that the integration of SDN to 5G networks requires a wireless SBi in which the controllers communicate with the data plane over a wireless channel. However, a wireless SBi is more complicated and suffers from other shortcomings such as radio interference. For instance, merely in terms of the latency on the SBi, the controllers will have to be placed closer to the switches, while this would increase the radio interference and the link failure probability. Note as well that the latency and link failure probability are probabilistic metrics and are more complicated to model.

Previous works by the authors [14], [18] discussed related works in the wired SDN domain. Other comprehensive surveys of the CPP solutions for wired SDNs can be found in [19]–[23]. In the following, the solutions are only reviewed for the CPP for wireless SDNs, which is the topic of this research.

The CPP for SDN was first introduced by Heller *et al*. [13]. They defined the CPP and the metrics for evaluating a solution for the initial placement of the control plane. The average propagation latency on the SBi, based on the Euclidean distance, was the main objective. The challenges and opportunities of Wireless Software Defined Networks (WSDN) were first suggested by Chaudet and Haddad [24].

The Wireless CPP (WCPP) was introduced by Abdel-Rahman *et al*. [25], [26] who initially proposed two different deterministic solutions for the CPP for wired SDNs and focused on the load of the control messages on the controllers. Their objective was to minimize the number of SDN controllers constrained by their response time and introduced the WCPP based on a Time Division Multiple Access (TDMA) mechanism where both the control plane and the SBi were wireless. In a different work Abdel-Rahman *et al*. [26] proposed a solution to the CPP in Software Defined Cellular Networks (SDCN) that considers the uncertainty in cellular user locations. They formulated a static joint stochastic controller placement and eNB-controller assignment problem to minimize the number of controllers needed to control all eNBs.

Kobo *et al*. [27] proposed the CPP for Software Defined Wireless Sensor Networks (SDWSN). Recently, Alharthi *et al*. [28] proposed a dynamic scheme for software defined drone networks. The objective of their solution is to minimize the number of drones that operate as SDN controllers and adjust their locations dynamically as the controlled nodes adjust their locations to meet changing mission requirements.

In previous works [14], [18] the authors proposed the WCPP for Wi-Fi based SDN networks where the SBi is a Wi-Fi based interface whose controllers communicate with the data plane APs using a Carrier Sense Multiple Access (CSMA) protocol. The communication between the controllers and the communication between the APs is also Wi-Fi based. Models for the wireless metrics (latency, link failure probability and transparency) were put forward and it was shown that their objective function minimizes the sum of these metrics on the SBi. In addition, it was shown by simulations that the solution to the WCPP is affected by these metrics.

This paper considers that in order to design an efficient wireless control plane it is necessary to perform a comprehensive investigation of the wireless metrics that affect the wireless SBi such as the Signal to Interference Ratio (SIR) and link failure probability. All the works above provide important insights into the solution for the WCPP, but they do not consider the building blocks of the wireless channel. Specifically, they do not examine the impact of the metrics of the wireless channel on the placement problem.

The conclusion of this section notes that the research of the CPP is increasingly being applied to wireless networks. However, none of the solutions have tackled the LTE-U case. The following presents the first optimization function and heuristics for the LTE-U-CPP case.

III. SYSTEM MODEL

Wang *et al*. [29] proposed a framework for a multi-Radio Access Technologies (multi-RAT) heterogeneous network which consist of an LTE-U tier and a Wi-Fi tier. This paper extends and adapts their work to model the wireless metrics of the proposed architecture.

Throughout this paper, $\mathbb{E}[X]$ is used to denote the expectation of a random variable X, $\mathbb{P}(A)$ to denote the probability of an event A, and $\mathcal{L}_X(\cdot)$ to denote the Laplace transform of a random variable X. The list of notations can be found in Table 3 (in Appendix B). The table includes a reference to the first appearance of each notation.

A. NETWORK MODEL

An LTE-U based WSDN network architecture is considered here. The network consists of multiple separate sub-networks where each of them is an LTE-U operator. Without loss of generality, in order to simplify the mathematical models it was decided to model two LTE-U operators. The architecture is composed of two logical parts: the data plane and the control plane. In the data plane, an LTE-U User Equipment (LUE) connects to the network through an LTE-U base station referred to as an eNB. The locations of eNBs are modeled by two independent homogeneous Poisson Point Processes (PPPs) for each operator; i.e., Φ_{L1} with density λ_{L1} and Φ_{L2} with density λ_{L2}. The LUE is also modeled as an independent PPP with density λ_{LU}.

Figure 1 depicts an example of the network model. $Operator_1$ has controller c_{11} that is assigned to eNBs e_{11}, e_{12}, e_{13} and controller c_{12} that is assigned to eNBs e_{14}, e_{15}. $Operator_2$ has controller c_{21} that is assigned to eNBs e_{21}, e_{22}, e_{23} and controller c_{22} that is assigned to eNBs e_{24}, e_{25}.

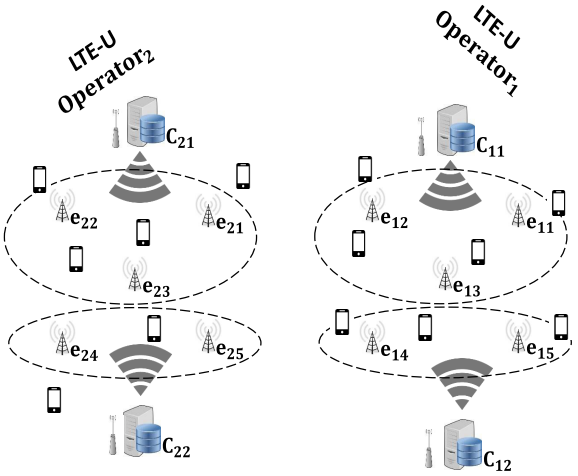

FIGURE 1. LTE-U-CPP network model.

Since the performance analysis and metrics formulation (Section IV) is similar for both operators, the notations Φ_L and λ_L are used, which refer to each of them. This is just to simplify the mathematical models. However, in the objective function (Equation (20)) each operator is represented by a different set of parameters. Therefore the required placement for the two LTE operators is independent. Hence, the simulation results show different placement and performance for the two operators (Figures 3, 6, 7).

In this paper the focus is on the downlink (DL) transmission since the traffic load in the DL is significantly higher than in the uplink (UL) [30]. In addition, in some technologies (e.g. in 4G) DL and UL are different in terms of MAC mechanism used. Therefore, it is difficult to introduce in the same paper and same model, parameters and mechanism that behave so differently. The UL justifies in itself an important future work.

The transmission power of an eNB is assumed to be fixed to a given value F_L and an LUE transmits in a given value F_U [29]. Both large-scale path loss and small-scale fading are considered. The power of a signal received by an LUE or an eNB located at a point y from an eNB, LUE or controller that is located at x is F_L |x-y|$^{-\alpha}$ h_{xy}. F_L is the transmission power of an eNB, |x-y| denotes the distance between x and y, $\alpha > 2$ is the path loss exponent, and h_{xy} denotes the channel power gain. The channel fading gain is considered to be independent and identically distributed (i.i.d.) across each link and each time slot, and to follow the exponential distribution with unit mean; i.e., Rayleigh fading. Since the focus of this paper is an interference-limited system, the background thermal noise is ignored.

All the network paths are assumed to be 1-hop; i.e., only direct paths from two network nodes are considered. The initial placement of the control plane is also investigated.

B. MAC MODEL

In the following, all eNBs are considered to have infinite backlog and operate in unlicensed band with slotted time. In order to avoid interference, LTE-U employs an ALOHA-like MAC scheme, where each eNB transmits independently with probability β_L in each time slot. U_{enb_i} denotes the retention indicator of the i^{th} eNB. The retention indicator of a given eNB is the probability that this eNB currently transmits and is defined as follows [29]

$$\mathbb{P}\left[U_{enb_i} = 1\right] = \beta_L \tag{1}$$

As such, $\widetilde{\Phi}_L$ which is the set of active eNBs in each time slot that form a thinned PPP and is defined as follows

$$\widetilde{\Phi}_L = \left\{x_i \in \Phi_L | U_{enb_i} = 1\right\} \tag{2}$$

where $\widetilde{\lambda}_L$ is the density and is defined as follows

$$\widetilde{\lambda}_L = \beta_L \lambda_L \tag{3}$$

Φ_L is the PPP of LTE-U.

IV. PERFORMANCE METRICS

In this paper stochastic geometry is used to model the network elements (controllers, eNBs and LUEs) as PPPs. Stochastic geometry is considered as a powerful mathematical tool to analyze cellular and Wi-Fi systems [31]–[34]. Therefore instead of calculating the average throughput and the average latency on the SBi, the spatial throughput and the spatial latency are calculated.

The performance metrics of an LTE-U network are: spatial link failure probability, spatial throughput, spatial latency and transparency defined as follows:

1) *Spatial link failure probability (SBi):* In the proposed model the transmitters on the SBi (Definition 1) are replaced by an equivalent continuum of transmitters which are spatially distributed in the network. This means that the transmitting power is now considered as a continuum field all over the SBi [35]. In this context, the network is characterised by eNBs and controllers density λ_L and LUEs density λ_{LU}. The LUEs are not part of the SBi but they create interference on the SBi. For eNBs, it is assumed that the transmission is successful if the received Signal to Interference Ratio (SIR) is above a predefined threshold. Let θ_L be the SIR threshold for eNB. The spatial link failure probability is then defined as (Section IV)
$$\overline{\mathbb{P}}_{\mathbb{L}} \triangleq \mathbb{P}[SIR < \theta_L] \tag{4}$$
2) *Spatial throughput (SBi):* In the literature, spatial throughput can also be referred to as area spectral efficiency [36]. Spatial throughput is a measure of how efficiently a limited frequency spectrum is utilized by the physical layer protocol, and sometimes by the media access control (the channel access protocol). For formal definition see Section IV-B.
3) *Spatial latency (SBi):* Only 1-hop paths between controllers and eNBs are considered. Therefore, the spatial latency on the SBi is straight forward from the spatial throughput.
4) *Transparency:* The transparency [14] is the marginal growth of the spatial latency on the data plane relative

to what it was before the introduction of the control plane (Section IV-D).

A. SPATIAL LINK FAILURE PROBABILITY FOR LTE-U

Let the typical eNB $enb_e \in \widetilde{\Phi}_L$ be located at the origin o and the assigned controller is c_L. The SIR at enb_e is given as

$$SIR = \frac{F_L \left|x_L\right|^{-\alpha} h_{c0}}{I_L + I_C + I_U} \tag{5}$$

where $|x_L|$ is the distance between enb_e and c_L. F_L is the transmission power of an eNB and h_{c0} is the channel power gain.

The LBT mechanism that is used prevents concurrent transmissions. However, it still does not guarantee complete protection from collisions since sensing of the medium is performed at exactly the same time, then it will still result in a collision.

I_L is the interference caused by the set of active eNBs except eNB enb_e and is defined as

$$I_L = \sum_{enb_{e_i} \in \widetilde{\Phi}_L \setminus enb_e} F_L \left|enb_{e_i}\right|^{-\alpha} h_{enb_{i0}} \tag{6}$$

where $\left|enb_{e_i}\right|$ is the distance between eNB enb_{e_i} and eNB enb_e. $h_{enb_{i0}}$ is the channel power gain. $\widetilde{\Phi}_L$ is the set of all active eNBs.

I_U is the interference caused by the set of all LUEs and is defined as

$$I_U = \sum_{lue_i \in \widetilde{\Phi}_U} F_U \left|lue_i\right|^{-\alpha} h_{lue_i 0} \tag{7}$$

where $|lue_i|$ is the distance between lue_i and eNB enb_e. $h_{lue_i 0}$ is the channel power gain and F_U is the transmission power of a LUE. $\widetilde{\Phi}_U$ is the set of all active LUEs.

I_C is the interference caused by the set of all controllers except for the controller $c_e = \eta(enb_e)$ that is associated with eNB enb_e and is defined as

$$I_C = \sum_{c_i \in C \setminus c_e} F_C \left|c_i\right|^{-\alpha} h_{enb_i 0} \tag{8}$$

$|c_i|$ is the distance between c_i and enb_e. $h_{enb_i 0}$ is the channel power gain.

Given the SIR threshold θ_L for the eNB, the spatial link failure probability of a typical eNB is given by [29]

$$\begin{aligned} \overline{\mathbb{P}}_{\mathbb{L}} &\triangleq \mathbb{P}[SIR < \theta_L] \\ &= \mathbb{E}_{|enb_L|}\left[\mathbb{E}_{U_{enb_L}}\left[\mathbb{P}\left[SIR_L < \theta_L \middle| \left|enb_L\right|, U_{enb_L}\right]\right]\right] \end{aligned} \tag{9}$$

U_{enb_L} is the retention indicator of an eNB enb_L. For a detailed formulation see Appendix A.

B. SPATIAL THROUGHPUT

The spatial throughput of LTE-U network is defined as [29]

$$R = \lambda_L \overline{P}_L \log\left(1 + \theta_L\right) \tag{10}$$

using Equation (9) the spatial throughput of LTE-U network is approximated by [29]

$$R \simeq \frac{\lambda_L \log\left(1 + \theta_L\right)}{\frac{1}{\beta_L} + \theta_L^{\left(\frac{2}{\alpha}\right)} \int_{\theta_L^{-\frac{2}{\alpha}}}^{\infty} \frac{1}{1+u^{\frac{\alpha}{2}}} du} \tag{11}$$

C. SPATIAL LATENCY

The purpose of the spatial latency used in this paper is mainly for calculating the transparency and evaluating the performance of the SBi. For this purpose only, a simpler definition for the spatial latency on the SBi is chosen, since only 1-hop paths between controllers and eNBs are considered.

$$L_s = \frac{1}{R} \tag{12}$$

D. TRANSPARENCY

If SDN is not considered, it is well known that the eNBs will only suffer from interference generated by other eNBs and LUEs. By contrast, when SDN is considered and controllers are deployed, the amount of interference on the data plane increases due to this new concurrent transmission, which impacts the spatial latency on the data plane. In other words, the introduction of the control plane affects the data plane since they coexist on the same spectrum. The transparency is the marginal growth of the spatial latency on the data plane relative to what it was before the introduction of the control plane. The density parameter of the entire network increases after installing the controllers from ν_1 to ν_2.

The spatial latency function of density ν is calculated based on Equation (10) where $\lambda_L = \nu$.

$$L\left(\nu\right) \triangleq L\left(\lambda_L = \nu\right) = \frac{\frac{1}{\beta_L} + \theta_L^{\frac{2}{\alpha}} \int_{\theta_L^{-\frac{2}{\alpha}}}^{\infty} \frac{1}{1+u^{\frac{\alpha}{2}}} du}{\nu \log\left(1 + \theta_L\right)} \tag{13}$$

Let ν_1 be the density parameter without the controllers i.e., the number of eNBs and LUEs per km^2. Let ν_2 be the density parameter on the network considering the controllers as well. Then, the transparency is defined as follows

$$T = \frac{L(\nu_2) - L(\nu_1)}{L(\nu_1)} \tag{14}$$

V. LTE-U CONTROLLER PLACEMENT PROBLEM

Consider a network represented by an undirected graph G (V,E) where V represents the set of network nodes: controllers, eNBs and LUEs. E represents the set of all wireless links. The set of controllers is denoted by C where $C \subseteq V$ and $C = \left\{c_{11}, .., c_{1k_1}\right\} \cup \left\{c_{21}, .., c_{2k_2}\right\}$ with k_1 and k_2 controllers for each operator respectively. The set of all eNBs is denoted by $E_n = \left\{enb_{11}, .., enb_{1m_1}\right\} \cup \left\{enb_{21}, .., enb_{2m_2}\right\}$ where m_1 and m_2 is the number of eNBs for the two operators and $E_n \subseteq V$. Since the network model for the two operators are identical, in the remainder of this paper the notation c_i, $1 \leq i \leq m$ is used for a controller. Each controller c_i is placed at a location denoted by $\psi(c_i)$. Therefore, a placement of

controllers is denoted by:

$$\Psi = \{(c_1, \psi(c_1)), (c_2, \psi(c_2)), \ldots, (c_k, \psi(c_k))\} \quad (15)$$

The set of all possible placements of controllers is denoted by $\widehat{\Psi}$. Denote the controller assigned to eNB enb_i by $\eta(enb_i)$. Denote by $\xi(c_i)$ the set of all eNBs that are assigned to controller c_i. An assignment function of eNBs to controllers is denoted by:

$$\Delta = \{(c_1, \xi(c_1)), \ldots, (c_k, \xi(c_k))\} \quad (16)$$

The set of all possible assignments of controllers to eNBs is denoted by $\widehat{\Delta}$. Equations (17) and (18) make sure that each eNB is assigned to exactly one controller.

$$\bigcup_{i=1}^{k} \xi(c_i) = E_n \quad (17)$$

$$\forall i, j \in \{1..k\}, \quad i \neq j \; \xi(c_i) \cap \xi(c_j) = \varnothing \quad (18)$$

A solution for the LTE-U-CPP is a set $\{k_1, k_2, \Psi, \Delta\}$ which consists of four elements:

1) k_1, k_2 are the minimal number of controllers for each operator.
2) Ψ is the optimal location of the controllers.
3) Δ is the assignment function of all eNBs to k clusters.

The set E is the sum of the following groups of wireless links:

1) wireless links between the controllers
2) wireless links between the eNBs
3) wireless links between each eNB and its assigned controller
4) wireless links between each LUE and its assigned eNB

Definition 1: The wireless SBi - denotes the wireless link between two network nodes x and y by (x, y). The set of wireless links on the SBi is defined as

$$\Lambda_{SBi} = \bigcup_{i=1}^{m} (\eta(enb_i), enb_i) \quad (19)$$

By definition the SBi does not include the links between eNBs, links between the controllers and the links between LUEs and the eNBs.

The objective is to find a placement Ψ for all controllers and assignment Δ between the controllers and the data plane network elements such that the sum of the link failure probability of the two operators $C_{1,1}$ and $C_{2,1}$, the spatial throughput $C_{1,2}$ and $C_{2,2}$ and the transparency $C_{1,3}$ and $C_{2,3}$ is minimized.

Based on the proposed network architecture and the aforementioned metrics, the objective function for the LTE-U-CPP can be modeled as shown in Eq. (20).

$$Minimize_{\Delta \in \hat{\Delta}, \Psi \in \hat{\Psi}} \sum_{i=1}^{2} \sum_{j=1}^{3} \left\{\lambda_{i,j} \cdot C_{i,j}(\Delta, \Psi)\right\} \quad (20)$$

$$\text{subject to:} \sum_{e \in E_n} x_{ec} \leq N_{ports}; \quad \forall c \in C \quad (21)$$

$$\sum_{c \in C} x_{ec} = 1; \quad \forall e \in E_n \quad (22)$$

$$\sum_{e \in \xi(c)} f(e) \leq \mu(e); \quad \forall c \in C \quad (23)$$

where $C_{i,j}$ and $\lambda_{i,j}$ are defined as follows. $C_{i,j}$ denotes the different metrics used in the objective function where $C_{1,1}$, $C_{2,1}$ are the spatial link failure probabilities for the two operators, $C_{1,2}$, $C_{2,2}$ stand for the spatial throughput metric and $C_{1,3}$, $C_{2,3}$ for the transparency. Since these metrics differ by nature it is necessary to introduce some coefficient parameters denoted by λ. These parameters define the impact of each performance metric on the results of the objective function. The exact dosage of these parameters is set by the operator with the following constraints:

$$-1 \leq \lambda_{i,j} \leq 1; \quad \forall\, 1 \leq i \leq 2,\ 1 \leq j \leq 3 \quad (24)$$

$$\sum_{i=1}^{2} \sum_{j=1}^{3} \lambda_{i,j} = 1 \quad (25)$$

It is noted that the spatial throughput should be maximized while the spatial link failure probability and the transparency should be minimized and therefore $\lambda_{1,2} < 0$ and $\lambda_{2,2} < 0$.

Constraint (21) guarantees that the number of eNBs that are assigned to controller c does not exceed c's port capacity N_{ports}. x_{ec} equals 1 if eNB e assigned to controller c and 0 otherwise. Constraint (22) guarantees that each eNB is assigned exactly one controller. Constraint (23) guarantees that the number of packets per second that must be sent to the controller, which is denoted by f(e) (for instance because there is no match on the eNB's look-up table), does not exceed the number of packets/second a controller can process, which is denoted by $\mu(c)$.

VI. HEURISTIC ALGORITHMS

The objective function (Equation (20)) uses six decision variables and three constraints, some of which are functions of stochastic variables. The placement problem is a K-Median problem which is already proved to be NP-Hard [37]. Therefore, a brute force or K-Median algorithm cannot solve this objective function in reasonable time even in a small number of network nodes. In addition, the K-Median algorithm is based on a hill-climbing search and since the objective function uses six decision variables with different behavior, the function may have several extremum points which make it impossible to solve with such an algorithm. Therefore, this section presents two heuristic approaches for solving the LTE-U-CPP. The first (Section VI-A) is a simulated annealing based algorithm, and the second (Section VI-B) is a Ray-Shooting based algorithm.

A. SIMULATED ANNEALING BASED ALGORITHM FOR THE LTE-U-CPP

To provide a fast solution, a simulated annealing based heuristic is proposed in this section. Simulated annealing is useful for finding a global optimum for problems that have a large search space and many local optima. It is based on a probabilistic method which was proposed independently by Kirkpatrick, Gelatt and Vecchi [38] as well as Cerny [39].

This algorithm was inspired by the metropolis algorithm for the cooling of materials by slowly lowering the temperature. In this algorithm worse solutions are also accepted with some probability. This way the algorithm will not stop at a local minimum when there is a different global minimum. This is done by using a control parameter known as temperature such that the probability of accepting worse solutions decreases with the temperature. Hence, it allows the algorithm to explore the search space at higher temperatures and helps in the convergence at lower temperatures. Furthermore, the probability of accepting worse solutions decreases with the difference between the objectives of the current and new solutions. The input to the algorithm is the network graph and the annealing schedule. The algorithm returns the best solution encountered during the traversal. For a proof of convergence see [40].

Algorithm 1 Clustering Algorithm Based on Hill Climbing With Simulated Annealing (HetNet-LTE-U-CPP-SA)

1: **Input:** $G(V, E)$, T_b, T_e, I_{max}, θ
2: **Output:** Ψ^{opt}, val^{opt}
3: $T \leftarrow T_b$, $val^{opt} \leftarrow inf$, $i \leftarrow 1$
   $\Psi \leftarrow$ RandomPlacement()
   val $\leftarrow$ PlacementEvaluation(Ψ)
4: **while** $T \geq T_E$ **do**
5: **if** (ConstraintsCheck(Ψ) = true) and ($val < val^{opt}$) **then**
   $\Psi^{opt} \leftarrow \Psi$, $val^{opt} \leftarrow val$
6: **end if**$\Psi' \leftarrow Neighbor(\Psi)$ using Alg. 2
   $val' \leftarrow PlacementEvaluation(\Psi')$
   $\Theta \leftarrow val' - val$
   $r \leftarrow$ random[0..1]
7: **if** $\mathbb{P}(\Psi', \Theta, T) \geq r$ **then**
8: $\Psi \leftarrow \Psi'$, $v \leftarrow val'$
9: **end if**$i \leftarrow i + 1$
10: **if** completed I_{max} iterations **then**
   $T \leftarrow T \cdot \theta$, $i \leftarrow 1$
11: **end if**
12: **end while**
   return Ψ^{opt}, val^{opt}

Algorithm 1 shows the LTE-U-CPP-SA, a simulated annealing based algorithm used to solve the objective function. The annealing schedule is limited by the starting temperature T_b and the ending temperature T_e (line 1). I_{max} iterations are made at each temperature and the temperature decrement is Θ. The algorithm begins with an initial temperature (line 3) and gradually decrements (line 10) until it reaches an ending temperature (line 4). The starting temperature must be selected very carefully; i.e, it should not be too high or too low. Generally, the starting temperature is set to 1 and the ending temperature is set to a small value such as 0.00001. In this case, the ending temperature was 10^{-10}. The ending temperature may not be zero because the probability of accepting the worst moves approaches zero as the temperature approaches zero. Then, the starting point is chosen randomly. In each iteration, the objective value and the constraints are calculated and compared to the current best solution (line 5). A better solution is chosen but a worse solution is also accepted with a probability $\mathbb{P}(Pl', \Theta, T)$ (line 8). Otherwise, another neighbor of the current solution is generated (line 6). The process continues until the temperature reaches an ending temperature. The simulated annealing parameters used in this paper are depicted in Table 1.

TABLE 1. Simulated annealing parameters.

$\mathbf{P}arameter$	$\mathbf{D}efinition$	$\mathbf{V}alue$
T_b	starting temperature	10^{-4}
T_e	ending temperature	10^{-8}
I_{max}	number of iterations	550
Θ	temperature decrement	0.95

Algorithm 2 Perturbation Operator for Simulated Annealing (SA-Perturb)

Input: G(V,E), Ψ(placement)
Output: $\Psi_{neighbor}$
C $\leftarrow$ set of all clusters
$c_n \leftarrow$ randomly chosen controller
$\gamma \leftarrow$ mutation factor close to zero
$\Omega \leftarrow$ Gaussian random number generator
Shift controller c_n by $\gamma \cdot \Omega$
Reassign all eNBs to controllers using
K-Nearest-Neighbor algorithm
$\Psi_{neighbor} \leftarrow$ new placement
return $\Psi_{neighbor}$

One of the most sensitive stages in the simulated annealing algorithm is choosing the perturbation of the current placement. A perturbed placement may consist of a change in controller number or a change in their location. Obviously, this results in a new assignment function of APs and eNBs to controllers. The current placement was perturbed by randomly adding or removing one controller and then choosing a controller and altering its placement using Gaussian mutation. After the perturbation, all the APs and eNBs were reassigned to their nearest controller using a K-NearestNeighbor algorithm. The perturbation operator is described in Algorithm 2.

Analysis and Discussion: Let n be the number of network elements (eNBs and controllers). LTE-U-CPP-SA goes through $\mathcal{O}$(logn) temperature steps. For each temperature, the search examines $\mathcal{O}$(n) attempted and accepted changes. The computation rejects a change of the current tour in $\mathcal{O}(1)$ time. If a change is accepted, the average path reversal involves $\mathcal{O}$(n) exchanges. Consequently, the run time T(n) of LTE-U-CPP-SA has the complexity:

$$T(n) = \mathcal{O}((n^2 + n) \cdot \log n) \tag{26}$$

Since most steps take place at low temperature, where most changes are rejected, the $\mathcal{O}$(n $\cdot$ log n) term is not negligible compared to the $\mathcal{O}(n^2 \cdot \log n)$ term.

The calculated running time complexity is generally considered as a fairly low complexity, and therefore the heuristic can be considered fast. For instance, Liu *et al*. [41] compared the running time of a simulated annealing based heuristic to an enumeration algorithm and showed that simulated annealing is more efficient.

B. RAY-SHOOTING BASED ALGORITHM FOR LTE-U-CPP

Peretz [42] proposed the Ray-Shooting (RS) heuristic algorithm for extracting static-output-stabilizing-feedback, with approximately minimal-norm, for Linear Time-Invariant (LTI) systems [43].

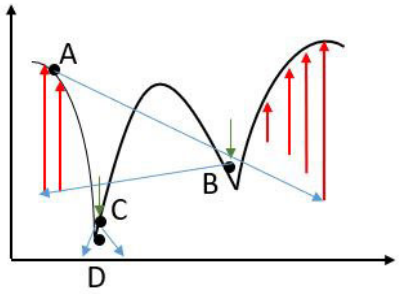

FIGURE 2. Ray-shooting algorithm.

Figure 2 shows an example of using the RS algorithm. The algorithm searches for the global minimum of the function y = f(x) in D. The algorithm starts at point A and ''shoots'' an arrow at a random angle α_1 until it intersects with the function f(x) at point B. Then, the algorithm ''shoots'' an arrow in the opposite direction at a random angle α_2 towards point C. This process continues until the algorithm converges up to a threshold ϵ close to point D. The Ray-Shooting works as follows (Figure 2): point A is chosen randomly on the graph of the function. From point A a random ray is shot towards the boundary of the search space. Starting from the ray head, the ray is sampled and the height of the function over the sampled points is compared to the height of the sampled points of the ray (the red and green vertical arrows). Once a lower point is reached - point B in the illustration - the ray sampling and function evaluations are stopped and a new random ray is shot from B in the opposite direction. The new ray is sampled and a lower function value at point C in the figure is found. Shooting rays from point C does not lead to any improvement greater than ϵ and the current iteration ends. Then, another iteration starts the same way and so on. The function f(x) may be of un-limited arguments and each argument is translated to a specific dimension in the ray's movement. In addition, multiple arrows can be shot in parallel. This is an advantage in a multi core system where each ray may be simulated in a different thread that is running on a different core. The algorithm is guaranteed to converge (in probability) to the global minimum of the function, if a sufficient number of iterations is allowed. Practically, the algorithm can be stopped if no improvement is detected within a window of 20% of the allowed number of iterations. The function need not be smooth or even continuous but only well defined and measurable over some compact domain, and the neighborhood of the global minimum value should have a non-negligible measure.

Further descriptions of the algorithm, the convergence proof and complexity calculations can be found in [44]–[46].

In this paper the RS algorithm was adapted to solve the proposed objective function. The LTE-U-CPP-RS heuristic based on the RS algorithm is proposed. The LTE-U-CPP-RS heuristic uses three rays for the three metrics in the objective function (Equation (20)).

The LTE-U-CPP-RS algorithm has two advantages that are important for the LTE-U-CPP:

1) An unlimited number of dimensions: the proposed objective function consists of three different metrics and the placement solution for the LTE-U-CPP consists of a location for the controllers and an assignment of eNBs to controllers. The proposed objective function was defined as multi-dimensional such that each metric and each location coordinate assignment function can be assigned a different dimension. This way, the search scheme simulated by shooting rays searches multiple variables concurrently. Hence, a solution for the LTE-U-CPP can be effectively calculated by the LTE-U-CPP-RS algorithm.
2) Multiple rays: The LTE-U-CPP-RS algorithm supports the use of multiple rays. The algorithm can ''shoot'' multiple rays in parallel, thus making the run time of the algorithm shorter. The simulation application can simulate multiple rays on multiple threads such that on a multi-core system the running time of the LTE-U-CPP-RS algorithm can improve significantly.

Section VII shows by simulations that the LTE-U-CPP-RS heuristic outperforms the LTE-U-CPP-SA heuristic.

VII. SIMULATION RESULTS

In this section, The LTE-U-CPP is solved with simulations of the two proposed algorithms LTE-U-CPP-SA and LTE-U-CPP-RS. The influence of the LTE-U metrics (latency, throughput, link failure probability and transparency) on the placement calculations of the LTE-U-CPP is evaluated. Unless otherwise specified, the transmission power of eNB and controller are assumed to be $F_L = F_C = 44dBm$, while the SIR threshold for eNB is $\theta_L = 0dB$. The transmission power of LUE is assumed to be $F_U = 23dBm$. The path loss exponent is $\alpha = 4$ [29], and the retention probability of eNB is $\beta_L = 1$ [29]. Intel Core i5-2400 CPU @ 3.10GHz, 3101MHz, 4 Cores, running Matlab RS2015a was used for the simulation.

The simulation area was 10 km × 10 km and the simulation results were averaged over 2000 iterations. The average results are presented for statistical reliability. The proposed LTE-U-CPP-SA and LTE-U-CPP-RS heuristics are evaluated on different sizes of networks. It was assumed that the controller software runs on a server with maximum access bandwidth of 10Gbps and capacity of $7.8 \cdot 10^6$ packets/second to serve 160 bytes packet size according to

TABLE 2. Simulation parameters.

Parameter	Description	Value
F_L	Transmission power - eNB	44dBm
F_L	Transmission power - controller	44dBm
θ_L	SIR threshold for eNB	0dB
F_U	Transmission power - LUE	23dBm
α	Path loss exponent	4
β_L	Retention probability - eNB	1
	Simulation area	10km X 10km
	Server maximum access bandwidth	10Gbps
	Controller capacity	$7.8 \cdot 10^6$

OpenFlow v 1.2 specifications [47]. The simulation parameters are depicted in Table 2.

A. REQUIRED NUMBER OF CONTROLLERS

One of the most important results of the LTE-U-CPP is the number of controllers that is required for the performance of the control plane. Although a large number of controllers means that the controllers are closer to the eNBs on average and the spatial link failure probability decreases, there is more interference and the SIR decreases.

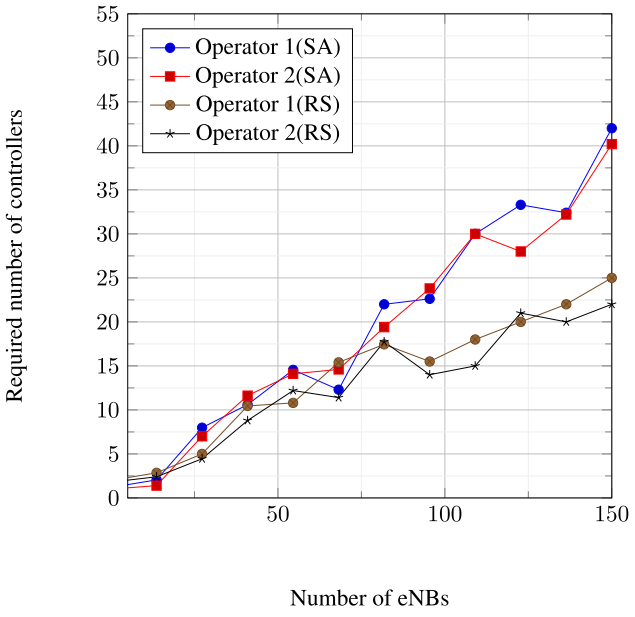

FIGURE 3. Required number of controllers vs. number of eNBs LTE-U-CPP-SA and LTE-U-CPP-RS.

Figure 3 shows the required number of controllers vs. the number of eNBs for both heuristics. In general the required number of controllers is seen to be greater for higher numbers of eNBs. However, adding a data plane node can increase or decrease the number of required controllers unpredictably because an additional network node adds interference to the network which changes all the wireless metrics (throughput, link failure probability, etc.) and the assignment of data plane nodes to controllers. Hence, the network configuration changes. For instance, the results of the SA heuristic show an unusual behaviour of the function for 70 and 110 eNBs was observed. A similar behaviour was observed by the results of the RS heuristic.

We observe that the LTE-U-CPP-RS calculates a lower number of controllers which is obviously closer to the optimum.

Summary: The LTE-U-CPP-RS heuristic calculates a lower number of controllers which is closer to the optimum..

B. OBJECTIVE VALUE

Figure 4 shows the objective value vs. the number of eNBs that was calculated by both heuristics. The error bars show the results variation of all the simulation iterations. In most network configurations the calculations of the LTE-U-CPP-RS heuristic are seen to produce lower objective values. This shows that the results of the LTE-U-CPP-RS heuristic are closer to the optimum.

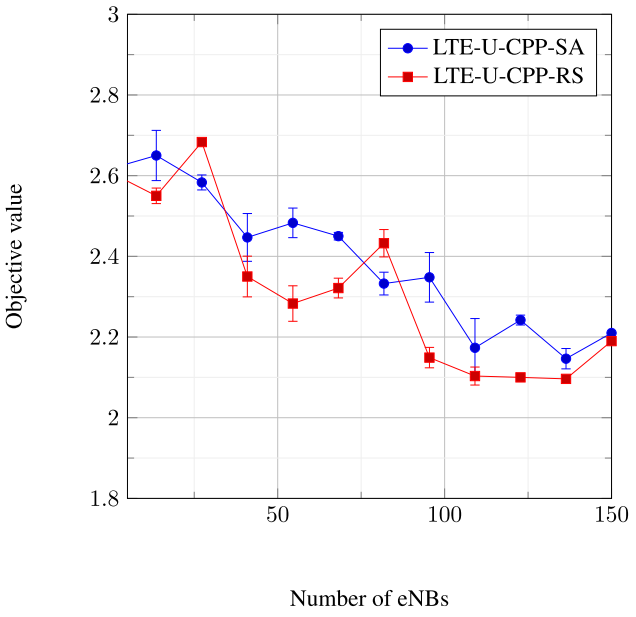

FIGURE 4. Objective value vs. number of eNBs.

Summary: The calculations of the LTE-U-CPP-RS heuristic have lower objective values.

C. SPATIAL THROUGHPUT

Figure 5 shows the spatial throughput vs. the number of eNBs for the two heuristics. The results deviate rapidly because every change in the data plane changes the structure of the network completely (the same behaviour was observed in Figure 3).

The LTE-U-CPP-RS heuristic appears to show smaller differences between the two operators. The results are more reliable since both operators have the same number of network elements in each instance of the simulations.

Summary: The results that are calculated by the LTE-U-CPP-RS are more reliable.

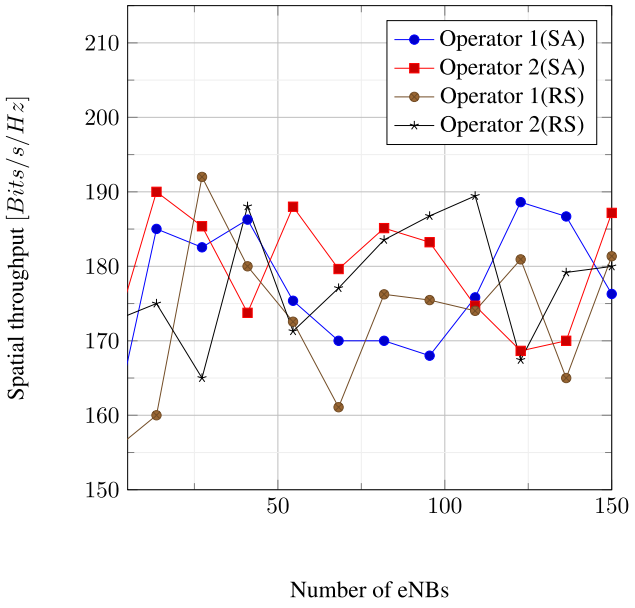

FIGURE 5. Spatial throughput vs. number of eNBs LTE-U-CPP-SA and LTE-U-CPP-RS.

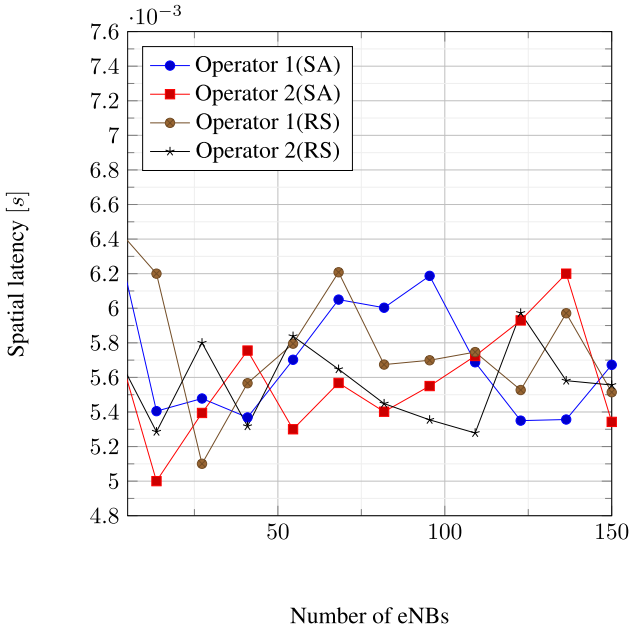

FIGURE 6. Spatial latency vs. number of eNBs LTE-U-CPP-SA and LTE-U-CPP-RS.

D. SPATIAL LATENCY

Figure 6 shows the spatial latency vs. the number of eNBs for the two heuristics. The results deviate rapidly because every change in the data plane changes the structure of the network completely (the same behaviour was observed in Figure 3).

The LTE-U-CPP-RS heuristic appears to show smaller differences between the two operators. The results are more reliable since both operators have the same number of network elements in each instance of the simulations.

Summary: The results that are calculated by the LTE-U-CPP-RS are more reliable.

E. TRANSPARENCY

The transparency is a measurement of the performance cost paid in installing the controllers. The controllers add interference on the data plane which reduces the SIR and increases the spatial latency.

Figure 7 shows the transparency of the required control plane placement vs. the number of eNBs for both heuristics. In general, the transparency appears to decay as the number of eNBs increases. This is because in large networks (more network nodes) the marginal interference that is added by an additional controller is less significant. Hence, the transparency is low. This is an interesting observation which shows that for larger networks the cost of using the wireless SDN architecture is lower. It is also observed that the LTE-U-CPP-RS calculates lower transparency.

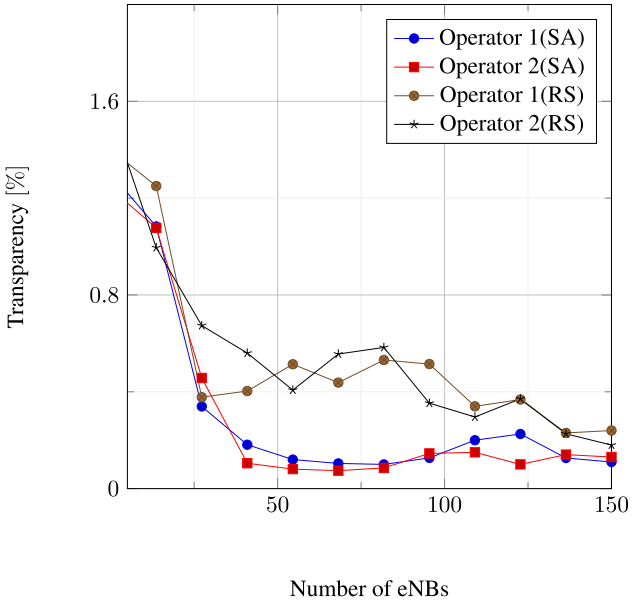

FIGURE 7. Transparency vs. number of eNBs LTE-U-CPP-SA and LTE-U-CPP-RS.

Summary: The transparency decays as the number of eNBs increases. The LTE-U-CPP-RS heuristic outperforms the LTE-U-CPP-SA by calculating lower transparency.

When the results of the LTE-U-CPP-SA heuristic are compared to the results of the LTE-U-CPP-RS heuristic the following is observed:

1) The two operators have the same density of eNBs and the same set of λ coefficient parameters in the objective function. The difference between the two operators lies in the scattering of the eNBs. In addition the probabilistic nature of the LTE-U-CPP-SA and the LTE-U-CPP-RS heuristics produces different results for the two operators. However, no major difference is expected. The spatial latency results of the LTE-U-CPP-RS heuristic in Figure 6 show practically similar results for the two operators, which is more accurate than the results of the LTE-U-CPP-SA heuristic.

TABLE 3. List of notations.

Parameter	Description	Value	Section
c	Controller		V
C	set of all controllers		V
$C_{i,1}$	link failure probability-objective function		V
$C_{i,2}$	spatial throughput-objective function		V
$C_{i,3}$	transparency-objective function		V
enb	eNB		IV
F_L	transmission power - eNB	44 dBm	III
F_C	transmission power - controller	44 dBm	III
F_U	transmission power - LUE	23 dBm	III
h	channel power gain		III
I_{max}	number of iterations		VI-A
lue	LUE		IV
L_s	spatial latency		IV
$L(\nu)$	spatial latency for a specific density of transmitters		IV-D
N_{ports}	ports capacity of a controller	const	IV
$\mathbb{P}_{\mathbb{L}}$	link failure probability		IV
R	spatial throughput		IV
SIR	signal to interference ratio		IV
T_b	starting temperature		VI-A
T_e	ending temperature		VI-A
U	retention indicator		III
α	attenuation factor	4	III
$\widetilde{\Phi}_L$	set of all active eNBs		III
$\widetilde{\Phi}_U$	set of all active LUEs		III
$\widetilde{\Phi}_{L_c}$	set of all controllers		III
Φ_L	homogeneous Poisson Point Processes (PPP) - LTE-U		IV
λ_L	eNBs and controllers density of homogeneous Poisson Point Processes (number of transmitters per km^2)		III
θ_L	threshold SIR for eNB	0 dB	III
θ_W	threshold SIR for AP	0 dB	III
β_L	retention probability of eNB	1	III
λ_{LU}	LTE-U user density		III
$\widetilde{\lambda}_L$	active eNBs in each time slot		III
$\lambda_{i,j}$	coefficient parameters	constant	V
Θ	temperature decrement		VI-A
Δ	assignment		V
$\widehat{\Delta}$	set of all assignments		V
Ψ	placement		V
$\widehat{\Psi}$	set of all placements		V
$\psi(c)$	location of a controller		V
ν	density of data plane nodes (number of transmitters per km^2)		IV
σ^p	number of messages per second produced by a data plane node	const	V

TABLE 3. *(Continued.)* **List of notations.**

Parameter	Description	Value	Section
μ^c	messages capacity of a controller	const	V
$\xi(c)$	set of all data plane nodes assigned to controller c		V
Λ_{SB_i}	the set of wireless links on the SBi		V
$\Gamma(\cdot)$	Gamma function		VI-A

2) The transparency is the marginal latency that the controllers add to the data plane. Therefore, the transparency is expected to be lower for larger networks. In Figure 7 the results of the LTE-U-CPP-RS heuristic show an emphatic decay compared to the results of the LTE-U-CPP-SA heuristic. In addition, the LTE-U-CPP-RS heuristic shows closer results for the two operators.
3) In Figure 7 the LTE-U-CPP-RS heuristic is shown to produce lower transparency.
4) The quality of the placements can also be measured by the number of controllers required. An accurate algorithm can calculate the optimum number of controllers precisely. Figure 3 shows that the LTE-U-CPP-RS heuristic calculates a lower number of controllers on average than the LTE-U-CPP-SA heuristic.
5) The most significant advantage of the LTE-U-CPP-RS heuristic over the LTE-U-CPP-SA heuristic is shown in Figure 4 where the objective values calculated by the LTE-U-CPP-RS heuristic are generally lower.

VIII. CONCLUSION AND FUTURE PLANS

To the best of our knowledge, this paper is presume to be the first to address the issue of the CPP for SDN based LTE-U networks. In the proposed network two LTE-U operators share the same LTE-U bandwidth.

The proposed objective function calculates the optimal placement for the control plane of both coexisting operators. In the objective function 3 metrics were considered: the spatial throughput, the spatial link failure probability and the transparency. Two heuristics were also presented to solve the objective function: a simulated annealing based algorithm LTE-U-CPP-SA and a ray-shooting based algorithm LTE-U-CPP-RS. The simulation results show that the LTE-U-CPP-RS heuristic calculates better and more accurate results than the LTE-U-CPP-SA heuristic.

For future work, the plan is to tackle the CPP problem in the case of heterogeneous LTE based networks for shared Wi-Fi and cellular technologies.

APPENDIX A
SPATIAL LINK FAILURE PROBABILITY FOR LTE-U

Given the SIR threshold θ_L for the eNB, the link failure probability of a typical eNB is given by [29]

$$\begin{aligned}\overline{\mathbb{P}}_{\mathbb{L}} &\triangleq \mathbb{P}[SIR < \theta_L] \\ &= \mathbb{E}_{|enb_L|}\left[\mathbb{E}_{U_{enb_L}}\left[\mathbb{P}\left[SIR_L < \theta_L \,|\, |enb_L|, U_{enb_L}\right]\right]\right] \\ &= \int_0^\infty \mathbb{P}[SIR < \theta_L \,|\, |enb_L| = \tau, U_{enb_L} = 1]\beta_L f_{|z_L|}(\tau)d\tau\end{aligned} \tag{27}$$

where

$$f_{|enb_L|}(\tau) = 2\pi\lambda_L \cdot \tau \cdot exp(-\pi\lambda_L\tau^2) \tag{28}$$

Therefore, the conditional link failure probability of the typical eNB is [29]

$$\begin{aligned}&\mathbb{P}[SIR < \theta_L \mid |enb_L|, U_{enb_L} = 1] \\ &\qquad = \mathcal{L}_{I_L||enb_L|,U_{enb_L}}\left(\frac{\theta_L\,|enb_L|^\alpha}{F_L}\right)\end{aligned} \tag{29}$$

Let $Z(s;a,b) = \pi(s\cdot a)^{\frac{2}{a}}\int_{b^2(s\cdot a)^{-\frac{2}{a}}}^\infty \frac{1}{1+u^{\frac{a}{2}}}du$, then
The conditional Laplace transform of I_L is given by [29]

$$\mathcal{L}_{I_L||enb_L|,U_{enb_L}}(s) = exp\left(-2\widetilde{\lambda_L}\int_{|z_L|}^\infty \frac{sF_L r^{-\alpha}}{1+sF_L r^{-\alpha}}rdr\right) \tag{30}$$

where $\widetilde{\lambda_L} = \beta_L\lambda_L$

By substituting $s = \frac{\theta_L|enb_L|^\alpha}{F_L}$, Eq. (30) into Eq. (29) one can obtain the conditional link failure probability. Then, by substituting Eq. (29) into Eq. (27), one can obtain the spatial link failure probability.

APPENDIX B
LIST OF NOTATIONS

See Table 3.

REFERENCES

[1] R. Yin, Y. Zhang, F. Dong, A. Wang, and C. Yuen, "Energy efficiency optimization in LTE-U based small cell networks," *IEEE Trans. Veh. Technol.*, vol. 68, no. 2, pp. 1963–1967, Feb. 2019.
[2] M. Gharbieh, A. Bader, H. ElSawy, H.-C. Yang, M.-S. Alouini, and A. Adinoyi, "Self-organized scheduling request for uplink 5G networks: A D2D clustering approach," *IEEE Trans. Commun.*, vol. 67, no. 2, pp. 1197–1209, Feb. 2019.
[3] T. LeAnh, N. H. Tran, D. T. Ngo, Z. Han, and C. S. Hong, "Orchestrating resource management in LTE-unlicensed systems with backhaul link constraints," *IEEE Trans. Wireless Commun.*, vol. 18, no. 2, pp. 1360–1375, Feb. 2019.
[4] J. Zhang, M. Wang, M. Hua, T. Xia, W. Yang, and X. You, "LTE on license-exempt spectrum," *IEEE Commun. Surveys Tuts.*, vol. 20, no. 1, pp. 647–673, 1st Quart., 2018.
[5] Y. Huang, Y. Chen, Y. T. Hou, W. Lou, and J. H. Reed, "Recent advances of LTE/WiFi coexistence in unlicensed spectrum," *IEEE Netw.*, vol. 32, no. 2, pp. 107–113, Mar. 2018.
[6] X. Wang, W. Chen, and Z. Cao, "ARCOR: Agile rateless coded relaying for cognitive radios," *IEEE Trans. Veh. Technol.*, vol. 60, no. 6, pp. 2777–2789, Jul. 2011.
[7] X. Wang, M. Sheng, D. Zhai, J. Li, G. Mao, and Y. Zhang, "Achieving bi-channel-connectivity with topology control in cognitive radio networks," *IEEE J. Sel. Areas Commun.*, vol. 32, no. 11, pp. 2163–2176, Nov. 2014.
[8] E. Alcatel-Lucent and S. Qualcomm, "Verizon LTE-U technical report coexistence study for LTE-U SDL v1. 0," LTE-U Forum, Alcatel-Lucent, Ericsson Qualcomm, Samsung, Tech. Rep., 2016.
[9] X. Ding, C.-H. Liu, L.-C. Wang, and X. Zhao, "Coexisting success probability and throughput of multi-RAT wireless networks with unlicensed band access," *IEEE Wireless Commun. Lett.*, vol. 5, no. 1, pp. 4–7, Feb. 2016.

[10] A. Jarwan, A. Sabbah, M. Ibnkahla, and O. Issa, "LTE-based public safety networks: A survey," *IEEE Commun. Surveys Tuts.*, vol. 21, no. 2, pp. 1165–1187, 2nd Quart., 2019.
[11] M. H. Rehmani, A. Davy, B. Jennings, and C. Assi, "Software defined networks-based smart grid communication: A comprehensive survey," *IEEE Commun. Surveys Tuts.*, vol. 21, no. 3, pp. 2637–2670, 3rd Quart., 2019.
[12] M. Patzold, *Mobile Fading Channels: Modelling, Analysis and Simulation*. Hoboken, NJ, USA: Wiley, 2001.
[13] B. Heller, R. Sherwood, and N. McKeown, "The controller placement problem," in *Proc. 1st Workshop Hot Topics Softw. Defined Netw. (HotSDN)*, 2012, pp. 7–12.
[14] A. Dvir, Y. Haddad, and A. Zilberman, "The controller placement problem for wireless SDN," *Wireless Netw.*, vol. 25, no. 8, pp. 4963–4978, Nov. 2019.
[15] G. Yao, J. Bi, Y. Li, and L. Guo, "On the capacitated controller placement problem in software defined networks," *IEEE Commun. Lett.*, vol. 18, no. 8, pp. 1339–1342, Aug. 2014.
[16] P. Vizarreta, C. M. Machuca, and W. Kellerer, "Controller placement strategies for a resilient SDN control plane," in *Proc. 8th Int. Workshop Resilient Netw. Design Modeling (RNDM)*, Sep. 2016, pp. 253–259.
[17] E. A. Mazied, M. Y. ElNainay, M. J. Abdel-Rahman, S. F. Midkiff, M. R. M. Rizk, H. A. Rakha, and A. B. MacKenzie, "The wireless control plane: An overview and directions for future research," *J. Netw. Comput. Appl.*, vol. 126, pp. 104–122, Jan. 2019.
[18] A. Dvir, Y. Haddad, and A. Zilberman, "Wireless controller placement problem," in *Proc. 15th IEEE Annu. Consum. Commun. Netw. Conf. (CCNC)*, Jan. 2018, pp. 1–4.
[19] B. Isong, R. R. S. Molose, A. M. Abu-Mahfouz, and N. Dladlu, "Comprehensive review of SDN controller placement strategies," *IEEE Access*, vol. 8, pp. 170070–170092, 2020.
[20] A. Kumari and A. S. Sairam, "A survey of controller placement problem in software defined networks," 2019, *arXiv:1905.04649*. [Online]. Available: http://arxiv.org/abs/1905.04649
[21] A. K. Singh and S. Srivastava, "A survey and classification of controller placement problem in SDN," *Int. J. Netw. Manage.*, vol. 28, no. 3, p. e2018, May 2018.
[22] J. Xie, D. Guo, Z. Hu, T. Qu, and P. Lv, "Control plane of software defined networks: A survey," *Comput. Commun.*, vol. 67, pp. 1–10, Aug. 2015.
[23] T. Hu, Z. Guo, P. Yi, T. Baker, and J. Lan, "Multi-controller based software-defined networking: A survey," *IEEE Access*, vol. 6, pp. 15980–15996, 2018.
[24] C. Chaudet and Y. Haddad, "Wireless software defined networks: Challenges and opportunities," in *Proc. IEEE Int. Conf. Microw., Commun., Antennas Electron. Syst. (COMCAS)*, Oct. 2013, pp. 1–5.
[25] M. J. Abdel-Rahman, E. A. Mazied, A. MacKenzie, S. Midkiff, M. R. Rizk, and M. El-Nainay, "On stochastic controller placement in software-defined wireless networks," in *Proc. IEEE Wireless Commun. Netw. Conf. (WCNC)*, Mar. 2017, pp. 1–6.
[26] M. J. Abdel-Rahman, E. A. Mazied, K. Teague, A. B. MacKenzie, and S. F. Midkiff, "Robust controller placement and assignment in software-defined cellular networks," in *Proc. 26th Int. Conf. Comput. Commun. Netw. (ICCCN)*, Jul. 2017, pp. 1–9.
[27] H. I. Kobo, A. M. Abu-Mahfouz, and G. P. Hancke, "Efficient controller placement and reelection mechanism in distributed control system for software defined wireless sensor networks," *Trans. Emerg. Telecommun. Technol.*, vol. 30, no. 6, p. e3588, Jun. 2019.
[28] M. Alharthi, A.-E.-M. Taha, and H. S. Hassanein, "Dynamic controller placement in software defined drone networks," in *Proc. IEEE Global Commun. Conf. (GLOBECOM)*, Dec. 2019, pp. 1–6.
[29] X. Wang, T. Q. S. Quek, M. Sheng, and J. Li, "Throughput and fairness analysis of Wi-Fi and LTE-U in unlicensed band," *IEEE J. Sel. Areas Commun.*, vol. 35, no. 1, pp. 63–78, Jan. 2017.
[30] G. Alfano, M. Garetto, and E. Leonardi, "New directions into the stochastic geometry analysis of dense CSMA networks," *IEEE Trans. Mobile Comput.*, vol. 13, no. 2, pp. 324–336, Feb. 2014.
[31] Y. Li, F. Baccelli, J. G. Andrews, T. D. Novlan, and J. C. Zhang, "Modeling and analyzing the coexistence of Wi-Fi and LTE in unlicensed spectrum," *IEEE Trans. Wireless Commun.*, vol. 15, no. 9, pp. 6310–6326, Sep. 2016.
[32] W. C. Cheung, T. Q. S. Quek, and M. Kountouris, "Throughput optimization, spectrum allocation, and access control in two-tier femtocell networks," *IEEE J. Sel. Areas Commun.*, vol. 30, no. 3, pp. 561–574, Apr. 2012.
[33] A. Rabbachin, T. Q. S. Quek, H. Shin, and M. Z. Win, "Cognitive network Interference- modeling and applications," in *Proc. IEEE Int. Conf. Commun. (ICC)*, Jun. 2011, pp. 1–6.
[34] J. Wen, M. Sheng, X. Wang, J. Li, and H. Sun, "On the capacity of downlink multi-hop heterogeneous cellular networks," *IEEE Trans. Wireless Commun.*, vol. 13, no. 8, pp. 4092–4103, Aug. 2014.
[35] J.-M. Kelif, M. Coupechoux, and P. Godlewski, "Spatial outage probability for cellular networks," in *Proc. IEEE GLOBECOM-IEEE Global Telecommun. Conf.*, Nov. 2007, pp. 4445–4450.
[36] M.-S. Alouini and A. J. Goldsmith, "Area spectral efficiency of cellular mobile radio systems," *IEEE Trans. Veh. Technol.*, vol. 48, no. 4, pp. 1047–1066, Jul. 1999.
[37] N. Megiddo and K. J. Supowit, "On the complexity of some common geometric location problems," *SIAM J. Comput.*, vol. 13, no. 1, pp. 182–196, Feb. 1984.
[38] S. Kirkpatrick, C. D. Gelatt, and M. P. Vecchi, "Optimization by simulated annealing," *Science*, vol. 220, no. 4598, pp. 671–680, 1983.
[39] V. Cerný, "Thermodynamical approach to the traveling salesman problem: An efficient simulation algorithm," *J. Optim. Theory Appl.*, vol. 45, no. 1, pp. 41–51, Jan. 1985.
[40] V. Granville, M. Krivanek, and J.-P. Rasson, "Simulated annealing: A proof of convergence," *IEEE Trans. Pattern Anal. Mach. Intell.*, vol. 16, no. 6, pp. 652–656, Jun. 1994.
[41] J. Liu, Y. Shi, L. Zhao, Y. Cao, W. Sun, and N. Kato, "Joint placement of controllers and gateways in SDN-enabled 5G-satellite integrated network," *IEEE J. Sel. Areas Commun.*, vol. 36, no. 2, pp. 221–232, Feb. 2018.
[42] Y. J. Peretz, "A randomized approximation algorithm for the minimal-norm static-output-feedback problem," *Automatica*, vol. 63, pp. 221–234, Jan. 2016.
[43] V. L. Syrmos, C. T. Abdallah, P. Dorato, and K. Grigoriadis, "Static output feedback—A survey," *Automatica*, vol. 33, no. 2, pp. 125–137, Feb. 1997.
[44] Y. Peretz, "On application of the ray-shooting method for LQR via static-output-feedback," *Algorithms*, vol. 11, no. 1, p. 8, Jan. 2018.
[45] Y. Peretz, "A randomized algorithm for optimal PID controllers," *Algorithms*, vol. 11, no. 6, p. 81, Jun. 2018.
[46] Y. Peretz, "On applications of the ray-shooting method for structured and structured-sparse static-output-feedbacks," *Int. J. Syst. Sci.*, vol. 48, no. 9, pp. 1902–1913, Jul. 2017.
[47] O. N. Foundation. *Interoperability Event Technical Issues Report*. [Online]. Available: https://3vf60mmveq1g8vzn48q2o71a-wpengine.netdna-ssl.com/wp-content/uploads/2014/10/openflow-spec-v1.2.pdf

AVIRAM ZILBERMAN received the bachelor's degree in software engineering from the Technion–Israel Institute of Technology, Haifa, Israel, in 1999, and the master's degree in computer science and mathematics from Ariel University, Ariel, Israel, in 2018, where he is currently pursuing the Ph.D. degree in the area of security in mobile ad-hoc networks with the Department of Computer Science.

YORAM HADDAD (Senior Member, IEEE) received the B.Sc. (Hons.), Engineer diploma (Hons.), and M.Sc. (radiocommunications) (Hons.) degrees from SUPELEC (leading engineering school), Paris, France, in 2004 and 2005, respectively, the Ph.D. degree (Hons.) in computer science and networks from Telecom ParisTech, in 2010, and the Habilitations (HDR) degree from Sorbonne University, in 2019. He was a Kreitman Postdoctoral Fellow with Ben-Gurion University, Israel, from 2011 to 2012. Since 2010, he has been a Faculty Member (currently at the rank of an Associate Professor) with the Jerusalem College of Technology (JCT)-Lev Academic Center, Jerusalem, Israel, and the Head of the FTNet Laboratory. He has published about 50 papers in international conferences (e.g., SODA), book chapters, and journals. His main research interests include wireless networks and algorithms for networks, wireless software defined networks (SDN), machine learning for 5G cellular networks and beyond, and lightweight security for IoT. He was a recipient of the Henry and Betty Rosenfelder Outstanding Researcher Award, in 2013, and the Computer Science Outstanding Lecturer Award, in 2018. He served on the Technical Program Committee for major IEEE conferences. He was the Chair of a working group at European COST action on Autonomous Control for a Reliable Internet of Services (ACROSS).

SEFI ERLICH received the B.Sc. and M.Sc. degrees in computer science from Ariel University, while more recently under Ariel's Cyber Center he later focused on algorithmic game theory under the supervision of Dr. Noam Hazon and Prof. Sarit Krus. He is currently working as a Data Scientist with private sector.

YOSSI (JOSEPH) PERETZ was born in Beer-Sheva, Israel, in 1963. He received the B.Sc. degree in mathematics and computer sciences, the B.Sc. degree in mechanical engineering, the M.Sc. degree in mathematics and computer sciences, and the Ph.D. degree in mathematics and computer sciences from the Ben-Gurion University of The Negev, Beer-Sheva, in 1988, 1995, 1995, and 1999, respectively. Since 1998, he has been a Senior Lecturer with the Lev Academic Center, Jerusalem College of Technology (JCT), Jerusalem, Israel. His research interests include control theory and its applications, optimization, randomized algorithms, parallel algorithms, linear algebra algorithms, complexity, computability, and cryptography.

AMIT DVIR received the B.Sc., M.Sc., and Ph.D. degrees from Ben-Gurion University, Beer Sheva, Israel, all in communication systems engineering. He is currently a Faculty Member with the Department of Computer Science and the Cyber Center, Ariel University, Israel. From 2011 to 2012, he was a Postdoctoral Fellow with the Laboratory of Cryptography and System Security, Budapest, Hungary. His research interest includes enrichment data from encrypted traffic.